ARTICLE

JMJD2 promotes acquired cisplatin resistance in non-small cell lung carcinoma cells

Lei Duan[1] · Ricardo E. Perez[1] · Paul D. Chastain II[2] · Mathew T. Mathew[3] · Divya Rani Bijukumar[3] · Carl G. Maki[1]

Abstract

Platinum-based drugs such as cisplatin (CP) are the first-line chemotherapy for non-small-cell lung carcinoma (NSCLC). Unfortunately, NSCLC has a low response rate to CP and acquired resistance always occurs. Histone methylation regulates chromatin structure and is implicated in DNA repair. We hypothesize histone methylation regulators are involved in CP resistance. We therefore screened gene expression of known histone methyltransferases and demethylases in three NSCLC cell lines with or without acquired resistance to CP. JMJD2s are a family of histone demethylases that remove tri-methyl groups from H3K9 and H3K36. We found expression of several JMJD2 family genes upregulated in CP-resistant cells, with JMJD2B expression being upregulated in all three CP-resistant NSCLC cell lines. Further analysis showed increased JMJD2 protein expression coincided with decreased H3K9me3 and H3K36me3. Chemical inhibitors of JMJD2-family proteins increased H3K9me3 and H3K36me3 levels and sensitized resistant cells to CP. Mechanistic studies showed that JMJD2 inhibition decreased chromatin association of ATR and Chk1 and inhibited the ATR-Chk1 replication checkpoint. Our results reveal that JMJD2 demethylases are potential therapeutic targets to overcome CP resistance in NSCLC.

Introduction

NSCLC accounts for about 80−85% of lung cancers. Standard NSCLC treatment includes platinum-based chemotherapy [1–3]. However, NSCLC has a low response rate to chemotherapy [2]. For patients that respond initially, acquired resistance occurs invariably [4]. Platinum drugs include cisplatin (CP), carboplatin, and oxaliplatin. CP interacts with purine bases in DNA to form DNA–protein and DNA–DNA interstrand and intrastrand crosslinks [5]. CP-mediated intrastrand DNA crosslinks are the major forms of DNA adducts, accounting for 85–90% of total lesions [6]. CP-induced

DNA damage triggers DNA damage response (DDR) and apoptotic pathways.

Mechanisms for CP resistance have been studied for many years. DNA repair and DDR pathways contribute to CP resistance in model cell systems and clinical patients [7]. For example, nucleotide excision repair (NER) regulated by ERCC-XFP is involved in repair of both intrastrand and interstrand crosslinks [8–10]. ERCC1 overexpression is associated with CP resistance in cell lines and clinical samples [11–13]. Translesion synthesis by a special group of DNA polymerases repairs CP-mediated interstrand crosslinks and is found to regulate CP resistance in cell lines and clinical samples [7, 14, 15].

DNA repair is coordinated by DDR pathways. The DNA damage response kinase atxia telangiectasia and Rad3-related (ATR) is a DDR orchestrator that plays a critical role in the cellular response to replication stress [16]. ATR is activated upon DNA replication fork stalling

✉ Carl G. Maki
Carl_Maki@rush.edu

1   Department of Cell & Molecular Medicine, Rush University Medical Center, Chicago, IL 60612, USA

2   Department of Health Sciences Education, University of Illinois College of Medicine at Rockford, Rockford, IL 61107, USA

3   Department of Biomedical Sciences, University of Illinois College of Medicine at Rockford, Rockford, IL 61107, USA

and then phosphorylates downstream substrates to induce replication checkpoints and promote fork repair [16]. ATR is activated by binding to single-strand (ss) DNA. ATR forms a complex with ATR interacting protein (ATRIP) that interacts with ssDNA-bound replication protein A (RPA) [17]. ATR phosphorylates and activates checkpoint kinase 1 (Chk1). Inhibition of ATR-Chk1 can increase CP-induced cell death in CP-resistant cancer cells [18–20], suggesting a role for the ATR-Chk1-mediated signaling pathway and the replication checkpoint to promote CP resistance.

DNA repair takes place within the context of chromatin structure. Chromatin structure is regulated by histone modifications such as phosphorylation, acetylation, and methylation. The role of histone modification in double strand break (DSB) repair has been widely studied. It is established that the repair of DSBs requires reorganization of chromatin and nucleosomes [21]. One typical example is phosphorylation of H2AX at serine 139 (γH2AX) that occurs at the DSB. γH2AX regulates nucleosome remodeling and other posttranslational histone modifications which are critical for subsequent recruitment and retention of repair factors for DSB repair [22, 23].

Histone methylation is a type of histone modification with attachment of mono-, di-, or tri-methyl groups to the exposed histone tails at nucleosomes and is regulated by large families of histone methyltransferases and demethylases. Recent studies have found histone lysine methylation plays a role in repair of DSBs. For example, histone 3 lysine 79 (H3K79) methylation and H4K20 dimethylation (me2) recruit the protein 53BP1 to chromatin at the DSB to promote repair [24–26]. H3K9 trimethylation (me3) stimulates TIP60 histone acetyltransferase activity at the DSB site, resulting in acetylation of histones and ATM kinase, the latter activating ATM to further stimulate γH2AX formation and DNA repair [27]. Histone demethylase KDM5A/JAR1D1A is recruited to DSBs where it demethylates H3K4me3 and promotes binding of repair proteins ZMYND8-NuRD complex to DSBs [28]. These findings have opened an avenue for understanding histone methylation in DNA repair.

We hypothesize histone methylation is involved in CP-induced DNA damage repair and CP resistance in NSCLC cells. We developed three CP-resistant NSCLC cell lines and compared mRNA levels of known histone methyltransferases and demethylases to that in parental cells. We found that JMJD2 demethylase family genes are upregulated and H3K9me3 and H3K36me3 levels are decreased in all resistant cell lines. Subsequent analysis of the cells found JMJD2 family proteins promote CP resistance by promoting recruitment of ATR and Chk1 to chromatin and maintaining the ATR-Chk1 replication checkpoint.

Results

NSCLC cells with acquired resistance to CP have increased expression of JMJD2s and decreased histone methylation. Inhibition of JMJD2s overcomes CP resistance

Histone methylation is promoted by methyltransferases and inhibited by demethylases [29, 30]. Histone methylation status affects chromatin structure [31]. DNA damage is often associated with chromatin remodeling that facilitates DNA repair machinery assembly at the DNA damage sites [32, 33]. Histone methylation has been demonstrated to play an important role in DSB repair [33]. We hypothesized that histone methylation changes may contribute to CP resistance in NSCLC cells. To test this, we designed a cell-based approach by comparing parental NSCLC cell lines to their CP-resistant derivatives. Three NSCLC cell lines (A549, H1703, and H1975) were exposed to increasing doses of CP and surviving cells expanded between each treatment. The derivatives (A549CPR, 1703CPR, 1975CPR) became resistant to CP, indicated by significantly increased colony-forming ability (Fig. 1a). Resistant cells also had decreased apoptosis in response to CP (indicated by reduced % sub-G1 cells) with significant increases in IC50 values for CP (Fig. 1b).

We next compared mRNA levels of known histone methyltransferases and demethylases in the parental and CP-resistant derivative cell lines when either untreated or 24 h after CP treatment. We focused on individual genes or gene families that were upregulated in all three CP-resistant cell populations. The results revealed three methyltransferase genes (*PRDM2, SETD7,* and *SETD1A*) (Fig. S1) and three demethylase genes (*KDM3A/JMJD1A, KDM4B/JMJD2B,* and *KDM6A/UTX*) (Fig. S2) upregulated in all three resistant cell populations compared to their parental controls. Previous studies have established a selective role for JMJD1A in demethylating H3K9me1/2, JMJD2 demethylating H3K9me3 and H3K36me3, and ubiquitously transcribed tetratricopeptide repeat X-linked protein (UTX) in demethylating H3K27me3 [30, 34, 35]. We used immunoblotting to ask if CP-resistant cells expressed higher protein levels of JMJD1A, JMJD2B, and UTX, and if there were corresponding changes in histone methylation. The results confirmed JMJD2B was expressed at higher levels in all three resistant cell populations compared to parental cells, both basally and after CP treatment (Fig. 2a). Immunoblotting also showed H3K9me3 levels are decreased in all three CP resistant cells compared to parental control cells (Fig. 2b), consistent with the increased expression of JMJD2B. In contrast, H3K36me3 was decreased in 1703CPR cells and 1975CPR cells compared to parental controls, but was not appreciably decreased in
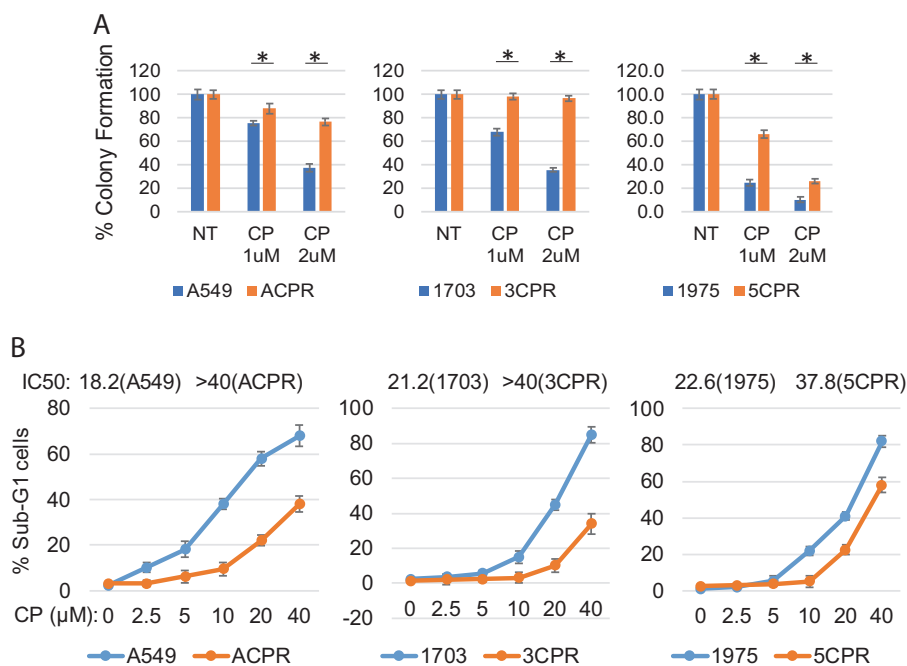
Fig. 1 NSCLC cells with acquired resistance to CP. **a** A549, H1703, H1975 cells and their CP-treated derivatives A549CPR (ACPR), 1703CPR (3CPR), and 1975CPR (5CPR) were plated in six-well plates in triplicate with 200 cells/well. The cells were treated with CP at the indicated doses for 48 h and then released of drugs. The cells were allowed to recover for 3 weeks to form colonies. Average percent colonies of the treated condition vs. control were presented with SD indicated. There is a significant difference between A549 and ACPR treated with 1 μM CP ($p = 0.036$) and 2 μM CP ($p < 0.01$), between H1703 and 3CPR treated with 1 μM CP and 2 μM CP ($p < 0.01$), between H1975 and 5CPR treated with 1 μM CP and 2 μM CP ($p < 0.01$). **b** 10^5 cells plated in six-well plates in triplicate and treated with different doses (2.5−40 μM) of CP for 24 h and then release of drugs for 48 h. Cells were analyzed with Flow Cytometry for sub-G1. Average percent sub-G1 cells were presented with SD indicated. There was a significant difference between parental and resistant cells in all three cell lines ($p < 0.01$). *$p < 0.05$

A549CPR cells vs. controls (Fig. 2b). UTX levels were increased basally and after CP treatment in 1703CPR and 1975CPR cells compared to parental control cells, but were not increased in A549CPR cells vs. controls (Fig. 2a). Consistent with increased levels of UTX that functions as a demethylase for histone H3K27 [36], H3K27me3 levels were decreased basally and after CP treatment in 1703CPR and 1975CPR cells compared to parental control cells (Fig. 2b). Finally, despite the apparent increase in JMJD1A mRNA levels in CP-resistant cells (Fig S1), JMJD1A protein was only basally higher in CP-resistant A549 and 1975 cells compared with their parental controls, and basal levels of the JMJD1A substrate H3K9me2 were slightly decreased (Fig. 2a, b).

UTX is encoded by an X-linked gene and is reported to have potential tumor suppressor activity [37]. In contrast, expression of JMJD2 family proteins has been linked to malignant transformation [38]. For example, JMJD2B and C amplification has been observed in medulloblastoma [39] and other cancers, and high expression of JMJD2B has been correlated with worse outcome in NSCLC patients [40]. JMJD2 inhibitors are being developed as potential therapeutic agents. In addition to JMJD2B expression being

increased in all three CP-resistant NSCLC cell lines, we also observed increased JMJD2D mRNA and protein expression in CP-resistant A549 and 1703 cells compared to parental controls (Fig. 2 and Supp Fig. 1). For these reasons we focused on JMJD2s as potential CP resistance factors in NSCLC cells. To test the role of JMJD2 proteins in CP resistance we utilized two different inhibitors: ML324 (selectively inhibits JMJD2 proteins) and JIB04 (inhibits JMJD2s, JMJD3, and JAR1D1A). Parental and CP-resistant cells were treated with CP and the inhibitors either alone or in combination, and long-term survival determined by colony formation ability. As shown in Fig. 3a, treatment with either CP or ML324 alone caused a relatively small reduction in survival (colony formation ability) in all three NSCLC cell lines and their CP-resistant derivatives, compared to combination treatment which reduced survival (colony formation) by 90−100%. Treatment with JIB04 alone caused a greater reduction in colony formation than did ML324 and when combined with CP reduced survival (colony formation ability) by nearly 100% (Fig. 3b). In addition, all the cells were treated with increasing doses of CP (2.5–40 μM) in the absence or presence of ML324 (20 μM) for 48 h and IC50 for CP-induced cell apoptosis
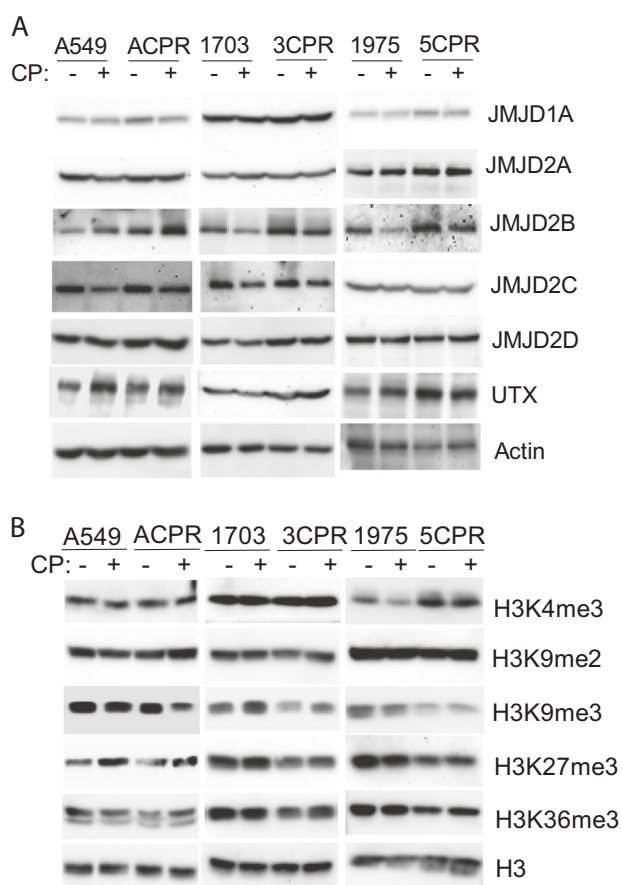
Fig. 2 Upregulation of JMJD expression in CP-resistant cells. a, b Parental A549, H1703, H1975 and CP-resistant A549CPR (ACPR), 1703CPR (3CPR), and 1975CPR (5CPR) cells were treated 24 h with CP (10 μM), lysates were immunoblotted for the indicated proteins

was determined. Notably, ML324 alone has minimal effect on apoptosis (<10%). However, ML324 significantly decreased the IC50 values of CP by approximately twofold in both parental and resistant cell lines (Fig. 3c). Immunoblotting showed increased H3K9me3 and H3K36me3 levels in cells cotreated with ML324 and CP, consistent with JMJD2 proteins being inhibited (Fig. 3d). Similarly, immunoblotting showed increased H3K9me3, H3K36me3, and H3K27me3 in cells cotreated with JIB04 and CP, consistent with inhibition of JMJD2 and JMJD3 family proteins (Fig. 3d). The results suggest inhibition of JMJD2s can increase CP sensitivity in NSCLC cells. Because JMJD2B expression was increased in all three CP-resistant cell populations, we tested if JMJD2B depletion could sensitize NSCLC cells to CP and if overexpression would have the opposite effect. Depletion of JMJD2B by siRNA in CP-resistant A549 cells increased H3K9me3 and H3K36me3 levels slightly (Fig. 3e) and also reduced survival (colony formation) compared to control cells (Fig. 3f). In contrast, JMJD2B overexpression partially reduced H3K9me3 and H3K36me3 levels in parental A549 cells

(Fig. 3g) and also increased survival (colony formation) in response to CP (Fig. 3h). These results suggest increased expression of JMJD2B alone can promote CP-resistance, at least to some extent, in NSCLC cells. Notably, depletion of JMJD2A or JMJD2D had no apparent effect on CP-induced cell death and survival (data not shown).

JMJD2 inhibition reduces ATR/Chk1 activation and ATR/Chk1 association with chromatin in CP-treated cells

The checkpoint kinase ATR plays a key role in the cell response to CP. ATR is activated in response to CP and then phosphorylates and activates downstream targets such as Chk1 to regulate cell cycle checkpoints and allow DNA repair and survival [16, 17]. We used the inhibitors ML324 and JIB04 as well as depletion of JMJD2B to address a possible role for JMJD2 proteins in ATR and Chk1 activation and signaling. As shown in Fig. 4a, ATR and Chk1 were activated by CP treatment in A549CPR and 1703CPR cells. This was indicated by increased ATR phosphorylation at T1989 (autophosphorylation site) and increased Chk1 phosphorylation at S345 (ATR phosphorylation site). Treatment with JIB04 or ML324 alone also increased ATR phosphorylation at T1989 and Chk1 phosphorylation at S345, though this effect was more pronounced with JIB04. This suggests JIB04 and ML324 themselves may induce replication stress and thus activate ATR and Chk1. Importantly, ML324 or JIB04 decreased ATR and Chk1 activation in CP-treated A549CPR and 1703CPR cells, while also increasing γH2AX (which indicates DSBs) (Fig. 4a, b). This suggests JMJD2 activity promotes or contributes to ATR and Chk1 activation and limits formation of DSBs in CP-treated cells. Depletion of JMJD2A, JMJD2B, or JMJD2D by siRNA also decreased ATR and Chk1 phosphorylation/activation in response to CP (Fig. 4c). Notably, JMJD2B depletion also increased γH2AX in response to CP-treated cells (Fig. 4c). Chk1 protein levels were decreased in response to CP in JMJD2A, JMJD2B, or JMJD2D knockdown cells while ATR protein was not changed (Fig. 4c). In contrast, transient overexpression of JMJD2B increased ATR activation and Chk1 phosphorylation while decreasing γH2AX in response to CP (Fig. 4d). The results suggest chemical inhibition of JMJD2 family proteins or depletion of JMJD2B specifically can reduce ATR activation and signaling to Chk1 in CP-treated NSCLC cells, leading to increased DNA DSB and increased killing.

We sought the mechanism for how JMJD2s could promote ATR/Chk1 activation and survival. JMJD2s modulate histone methylation which, in turn, could alter the accessibility to chromatin of factors such as ATR that require chromatin association to be activated. We therefore

A

■ A549 ■ ACPR   ■ 1703 ■ 3CPR   ■ 1975 ■ 5CPR

B

■ A549 ■ ACPR   ■ 1703 ■ 3CPR

C

IC50 (µM)	CP	CP+ML
A549	18.2	9.4
ACPR	>40	21.6
H1703	21.2	11.4
3CPR	>40	20.8
H1975	22.6	13.6
5CPR	37.8	15.8

D

1703CPR

E

ACPR

G

A549

F

■ A549 ■ ACPR

H
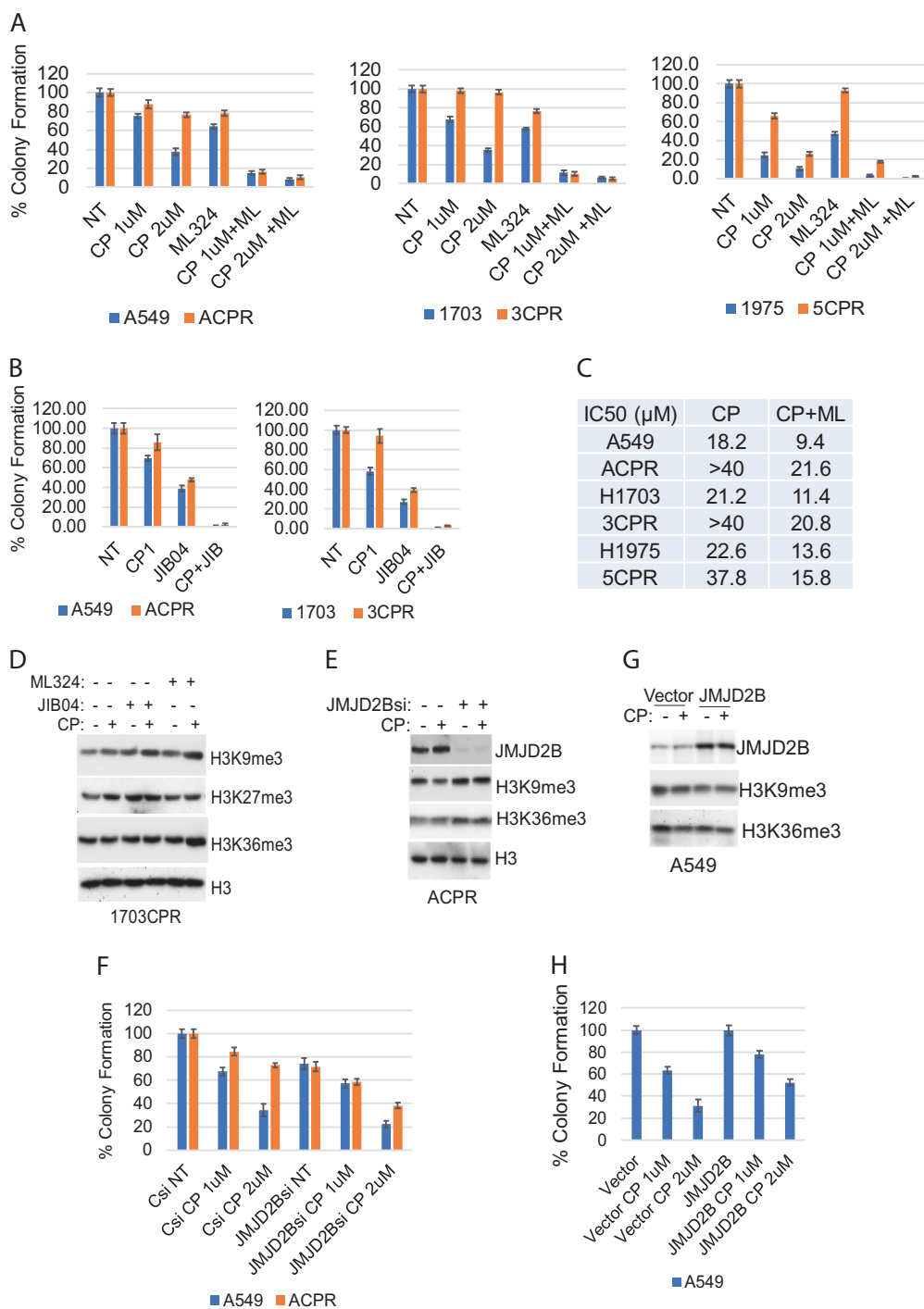
■ A549

monitored ATR chromatin association in cells treated with CP alone or CP plus the JMJD2 inhibitor ML324. As shown in Fig. 5a, b, total ATR and pATR association with chromatin was increased in CP-resistant A549CPR and 1703CPR cells treated with CP alone. However, the amount of total ATR and pATR associated with chromatin was decreased in cells cotreated with CP plus ML324. Chk1 chromatin association was also increased in CP-treated cells but less so in cells cotreated with CP plus ML3243

(Fig. 5a, b). Furthermore, knockdown of JMJD2B also decreased chromatin-associated ATR and Chk1 in response to CP (Fig. 5c). We noticed that in addition to decreased phosphorylation of Chk1 in cells with inhibition of JMJD2 (Fig. 4a), total levels of Chk1 were also decreased compared to control cells (Fig. 4). Because dissociation of Chk1 from chromatin in response to DNA damage is accompanied by ubiquitination and degradation of Chk1 [41], we speculated Chk1 maybe degraded in cells with inhibition of

◀ **Fig. 3** Inhibition of JMJD2 or knockdown of JMJD2B sensitizes cells to CP. Overexpression of JMJD2B makes cells resistant to CP. **a**, **b** Parental A549, H1703, H1975 and CP-resistant A549CPR (ACPR), 1703CPR (3CPR), and 1975CPR (5CPR) cells were plated on six-well plates (200 cells/well) in triplicate and treated with 1 or 2 µM CP and/or ML324 (5 µM) (**a**), or 1 µM CP and/or JIB04 (1 µM) for 48 h and then released of drugs. The cells were allowed to recover for 3 weeks for colony formation. Average percentages of colonies are presented with SD indicated. There are significant differences ($p < 0.05$) between CP and CP plus ML324 (or JIB04) and between ML324 (or JiB04) and CP plus ML324 (or JIB04) conditions in all three parental and CP-resistant cell lines. **c** The indicated cell lines were treated with different doses of CP ($2.5-40$ µM) in the absence or presence of ML324 (20 µM) for 24 h and then released of CP for 48 h. Average percentages of sub-G1 cells were used to calculate IC50s of CP for each cell line and condition which are presented. **d** 1703CPR cells were treated with CP and/or ML324 or JIB04 for 24 h. Lysates were immunoblotted for the indicated proteins. **e** ACPR cells were transfected with control siRNA or JMJD2B siRNA and then treated with CP (10 µM) for 24 h. Lysates were immunoblotted for the indicated proteins. **f** ACPR cells in six-well plates (200 cells/well) were transfected with control siRNA or JMJD2B siRNA and then treated with CP (1 or 2 µM) for 24 h and then released of drugs. The cells were allowed to recover for 3 weeks for colony formation. Average percentages of colonies are presented with SD indicated. There are significant differences between CP-treated control siRNA and JMJD2BsiRNA A549CPR (ACPR) cells ($p < 0.01$). There is no difference between 1 µM CP-treated control siRNA and JMJD2BsiRNA in A549 cells ($p > 0.05$). There is a significant difference ($p < 0.05$) between 2 µM CP-treated control siRNA and JMJD2B siRNA in A549 cells. **g** A549 cells were transfected with vector or JMJD2B plasmid. The cells were selected with puromycin and establish a bulk line. Vector expressing cells and JMJD2B expression cells were treated with CP (10 µM) for 24 h. Lysates were immunoblotted for the indicated proteins. **h** Cells expressing vector or JMJD2B in six-well plate (200 cells/plate) were treated with CP (1 µM or 2 µM) for 24 h and then released of drugs. The cells were allowed to recover for 3 weeks for colony formation. Average percentages of colonies are presented with SD indicated. There are significant differences ($p < 0.05$) between CP) (both 1 and 2 µM)-treated vector and JMJD2B A549 cells

JMJD2. To test that, we analyzed mRNA levels and protein degradation in cells treated with ML324 or JIB04. The results show Chk1 mRNA was slightly increased with CP treatment but not decreased by ML324 or JIB04 (Fig S3A). Importantly, ML324 induced a loss of Chk1 protein but not mRNA upon inhibition of protein synthesis by cycloheximide (CHX) for 4 h, suggesting Chk1 is degraded in cells with inhibition of JMJD2 (Fig. S3B and C). Chk1 is known to be degraded by Cul1/Cul4A ubiquitin ligases [41], which could be a mechanism for ML324-induced degradation of Chk1. We treated cells with ML324 in the absence or presence of MG132 for 4 h and then examined Chk1 ubiquitination and association with Cul4A by immunoprecipitation. Ubiquitinated Chk1 accumulated in MG132-treated cells that was slightly increased by cotreatment with ML324 (Fig. S3D), suggesting ML324 increases Chk1 ubiquitination. Cul4A coimmunoprecipitated with Chk1 in MG132-treated cells and this was also modestly increased by treatment with ML324/MG132 (Fig. S3E). This suggests

decreased Chk1 levels in JMJD2 inhibitor-treated cells could result from Cul4A-mediated degradation, at least in part. Altogether, these results suggest JMJD2 activity can promote or enhance ATR and Chk1 association with chromatin and in this way may increase ATR activation and maintain Chk1 stability in CP-treated cells.

JMJD2 inhibition inhibits the ATR-Chk1 replication checkpoint in CP-treated cells

CP causes replication stress by promoting DNA crosslinks that stall progression of DNA replication forks. Activated ATR and Chk1 promote survival by blocking restart and preventing collapse of stalled replication forks, and by inhibiting inappropriate activation of nascent replication origins [42–45]. Current models suggest that, when ATR and Chk1 activity is compromised, fork collapse and inappropriate replication origin firing leads to an excess of ssDNA that is potentially lethal unless bound by RPA. When it exceeds the pool of available RPA, ssDNA is left unbound and susceptible to cleavage, resulting in massive amounts of DNA breaks that can be visualized as pan-nuclear γH2AX staining. We used four markers to determine if ML324 inhibits the ATR-Chk1 replication checkpoint in CP-treated cells. First, RPA proteins bind ssDNA and therefore chromatin association of RPAs is a surrogate marker for ssDNA. We observed a pronounced increase in the amount of chromatin-associated RPA2 in cells treated with CP plus ML324 compared to either CP or ML324 alone (Fig. 5a, b). This is consistent with loss of the ATR-Chk1 replication checkpoint in CP plus ML324-treated cells leading to an increase in ssDNA.

Second, we used a DNA fiber assay to ask if ML324 alters replication fork restart and origin firing in CP-treated cells. In this assay cells are pulsed with IdU to label active replication forks, treated with CP and/or ML324 for 12 h, and then labeled with CldU (Fig. 6a, b). DNA fibers are isolated and stained with antibodies for IdU (visualized red) and CldU (visualized green). Contiguous red and green fibers represent replication forks that restarted after CP treatment, whereas only green fibers represent new origin firing. Untreated cells served as controls. CP treatment reduced replication fork restart (Fig. 6c), as expected for cells with ATR-Chk1 activation. However, fork restart was increased in cells treated with ML324 or CP+ML324 compared to cells treated with CP alone. Moreover, the length of red-green tracks was also increased in ML324- and CP+ML324 treated cells compared to cells treated with CP alone (Fig. 6e). New origin firing was also reduced by CP treatment but increased by ML324 or CP+ML324 (Fig. 6d). These results are consistent with ML324 reducing Chk1 activation leading to increased fork restart and increased origin firing in CP-treated cells. FACS analysis

Fig. 4 JMJD2 promotes ATR and Chk1 activation and decreased DNA damage in response to CP. **a, b** A549CPR (ACPR) and 1703CPR (3CPR) cells were treated with vehicle or CP (10 μM) with or without ML324 (20 μM) or JIB04 (2 μM) for 24 h. Lysates were immunoblotted for the indicated proteins. **c** ACPR cells were transfected with control siRNA or JMJD2A/2B/2D siRNA and then treated with CP (10 μM) for 24 h. Lysates were immunoblotted for the indicated proteins. **d** H1299 cells were transfected with vector or JMJD2B and then treated with (10 μM) for 24 h. Lysates were immunoblotted for the indicated proteins
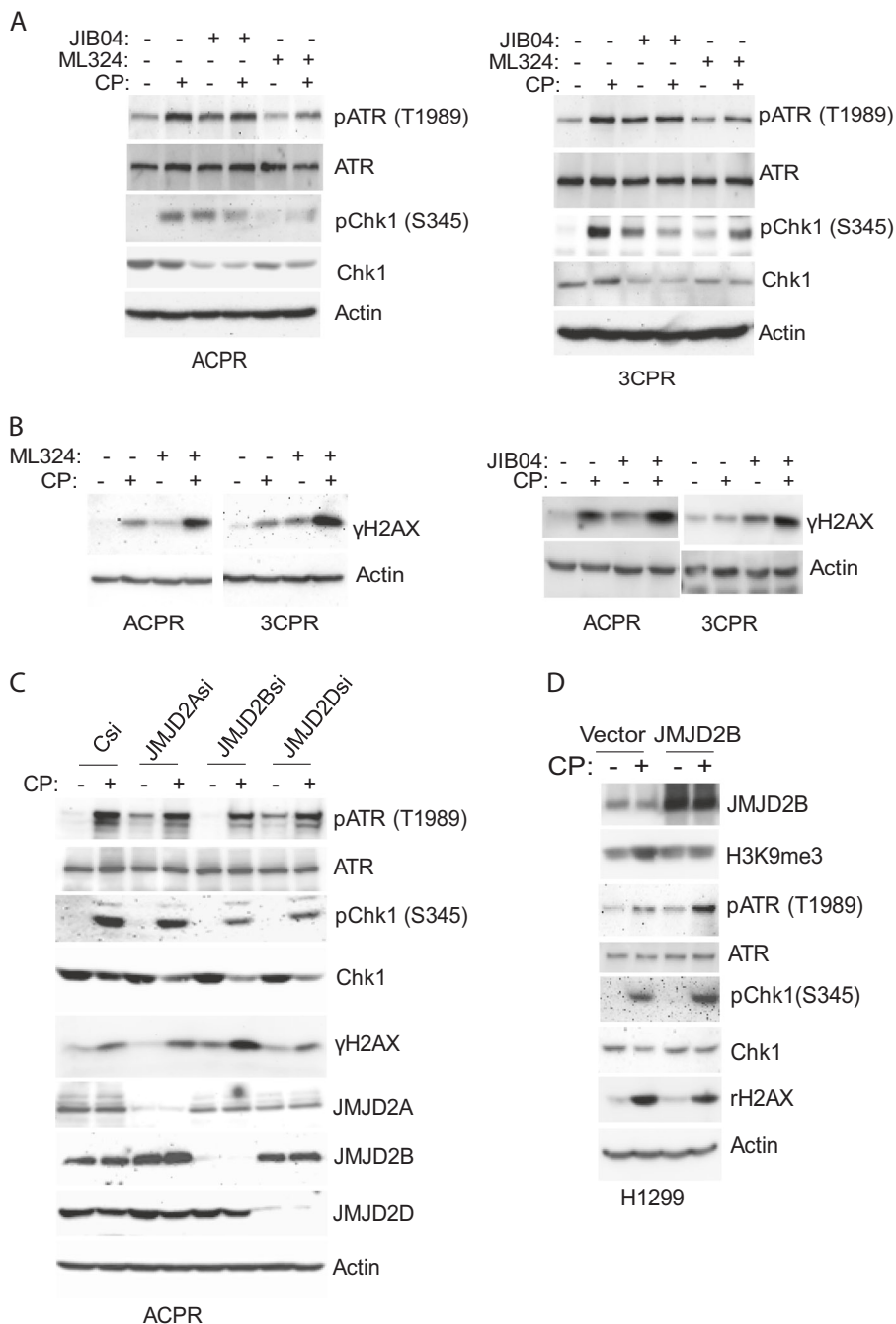
indicated cells treated with CP alone could progress slowly through S-phase and into G2/M phase while cells treated with CP+ML324 were S-phase arrested (Fig. S4). This suggested that replication progression is arrested by ML324 despite fork restart is increased (Fig. 6c, e). We again used a double labeling experiment to test this. Briefly, cells were pulsed with BrdU for 1 h to label S-phase cells, and then treated with CP or CP+ML324 for 6 h. CP was then removed and cells were cultured in EdU for 6, 16, or 24 h. BrdU and EdU double-labeled cells were gated and cell cycle profiles determined by 7-AAD staining. As shown in

Fig. 6f, g, BrdU/EdU double-labeled cells progressed out of S-phase after 24 h and into G2/M in cells treated with CP alone. In contrast, the same cells treated with CP+ML324 remained in S-phase and did not accumulate in G2/M (Fig. 6f, g). The results indicate ML324 arrests CP-treated cells in S-phase despite increasing replication fork restart and despite increasing new origin firing.

Next we examined γH2AX staining in cells treated with CP alone or CP+ML324/JIB04. We observed a large increase in pan-nuclear γH2AX staining, indicative of massive amounts of DNA breaks, in cells treated with CP

Fig. 5 Inhibition of JMJD2 decreases Chromatin-associated ATR and Chk1 and increases chromatin association of RPA. A549CPR (ACPR) (**a**) and 1703CPR (3CPR) (**b**) cells were treated with CP (10 μM) and/or ML324 (20 μM) for 24 h. **c** A549CPR (ACPR) cells were transfected with control siRNA or JMJD2B siRNA and treated with CP (10 μM) and/or ML324 (20 μM) for 24 h. Subcellular protein fractions of cytoplasm, nucleoplasm and chromatin were immunoblotted for the indicated proteins (Rb is a marker of nucleoplasm and H3 is a marker of chromatin)
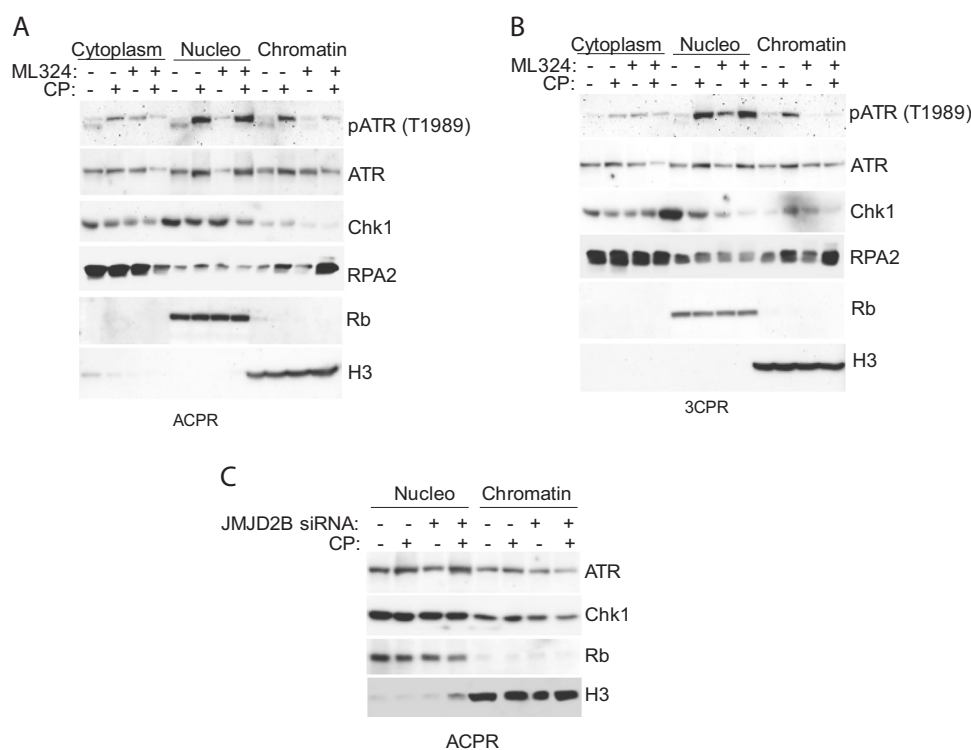
plus ML324 or JIB04 (Fig. 7a, b). This pan-nuclear γH2AX staining is consistent with abundant DNA breaks associated with loss of the ATR-Chk1 replication checkpoint.

Finally, to ask if unscheduled DNA origin firing is required for DNA breaks and/or death in CP plus ML324-treated cells, we used the cdc7 inhibitor XL413 which is shown to suppress firing of silent origins [46]. We found cotreatment with XL413 reduced γH2AX levels in cells treated with CP plus ML324 and also partially restored survival (Fig. 8a, b), which is consistent with the finding of Mutreja et al. [46] that inhibition of ATR-induced γH2AX is reversed by XL413 [46]. This result supports the idea that DNA breaks and death in cells treated with CP plus ML324 requires DNA replication origin firing and is consistent with ML324 causing loss of the ATR-Chk1 replication checkpoint.

Discussion

Cisplatin kills cancer cells by promoting intra- and inter-strand DNA crosslinks that induce replication stress and DNA damage [47]. The ATR checkpoint kinase plays an important role for repair of CP-induced DNA damage [48]. ATR is recruited to stalled replication forks and then activates downstream pathways for DNA repair [49]. Inhibition of ATR and its downstream effector Chk1 can sensitize cancer cells to CP [50], supporting the idea that the ATR-Chk1 pathway promotes CP resistance. Activation of ATR signaling pathways and assembly of repair machinery occur within the context of chromatin. Changes in chromatin structure and compaction are important for recruitment of DDR and repair proteins to the sites of damage [32, 33]. In this study, we found JMJD2 histone demethylases, that modulate chromatin structure and compaction by demethylating H3K9me3 and H3K36me3, play an important role in CP resistance by promoting the chromatin recruitment and activation of ATR and Chk1, and that targeting JMJD2s can overcome CP resistance in NSCLC cells.

We used three NSCLC cell lines and their CP-resistant derivatives to screen for gene expression differences of known histone methyltransferases and demethylases. JMJD2 family genes were found upregulated in all three resistant cell lines. Protein expression analysis confirmed that JMJD2B is upregulated in all three resistant cell lines and JMJD2A, JMJD2C, and JMJD2D are also variously upregulated across the resistant cell lines. Notably, JMJD2B is further upregulated in response to CP in WT p53-expressing A549 cells, which is consistent with JMJD2B being a p53 target gene. However, in mutant p53-expressing H1703 and H1975 cells, JMJD2B protein levels were decreased in response to CP. We speculate that JMJD2B protein is turned over in response to CP as JMJD2B was shown to be ubiquitinated and degraded at DNA damage sites [51]. JMJD2 family proteins remove tri-methylations from histone H3 lysines 9 and 36 (H3K9me3 and H3K36me3) [34]. Consistent with the upregulation of JMJD2, basal H3K9me3 and H3K36me3 levels were downregulated in all three resistant cell lines. Inhibition of
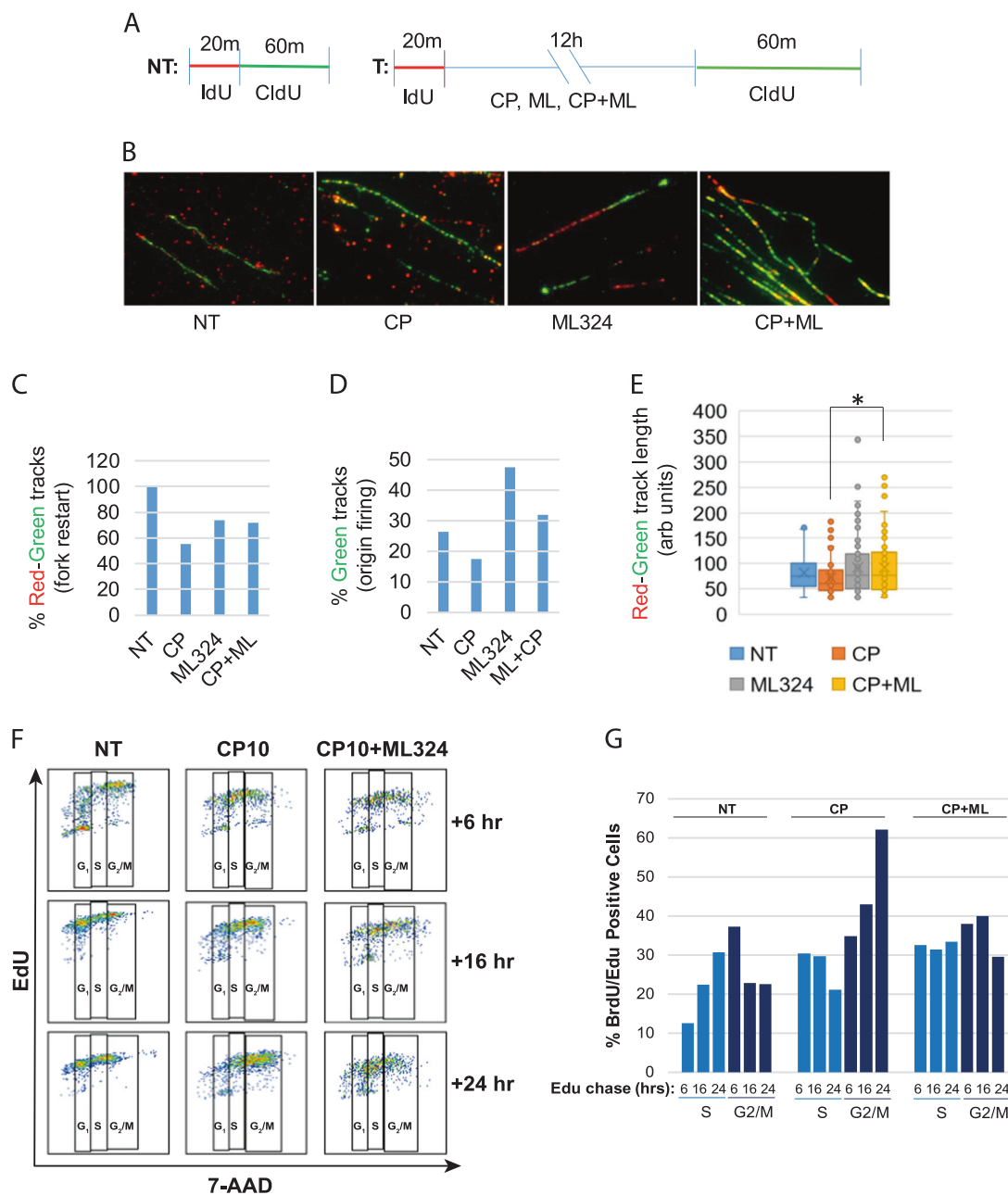
Fig. 6 Inhibition of JMJD2 increases origin firing and fork reinitiation but stalled replication of restarted forks. **a** Schematic presentation of IdU and CldU labeling and drug treatment of A549 cells for DNA fiber assay. NT no treatment, T treatment. **b** Representative images for DNA fibers acquired by immunofluorescent confocal scanning. Totally 1301 (NT), 2369 (CP), 2465 (ML324), and 2436 (CP+ML324) fibers including red (IdU) only, green (CldU) only, red-green, green-red-green, and red-green-red were analyzed. Percentages of red-green (fork restart) fibers in drug-treated conditions relative to control (NT) are presented (**c**). Percentages of green-only (origin firing) fibers relative to total fibers in each condition are presented (**d**). **e** Length of red-green (active forks) DNA fibers (totally 69 for NT, 69 for CP, 105 for Ml324, and 100 for CP+ML324) was measured and presented as a graph. There are significant differences among groups ($F = 3.05$, $p = 0.028$). There is a significant difference between CP and CP+ML324 ($p = 0.005$). There is no difference between NT and CP ($p = 0.12$), NT and ML324 ($p = 0.16$), and NT and CP+Ml324 ($p = 0.17$). **f** A549 cells were prelabeled with BrdU, treated with drugs, and then chased with EdU for the indicated times. BrdU-positive cells were gated and analyzed for EdU and cell cycle (7-AAD). Percentages of BrdU/EdU double-positive (forks restarted) cells in S and G2/M at the indicated times are presented

JMJD2s by JIB04 and ML324 increased H3K9me3 and H3K36me3 levels and sensitized resistant cells to CP. Knockdown of JMJD2B also partially sensitized resistant cells to CP. These results suggest JMJD2 family proteins promote CP resistance by decreasing H3K9me3 and H3K36me3. It is noteworthy that in two of the three resistant cell lines (1703CPR and 1975CPR) UTX was also upregulated which coincided with decreased levels of

Fig. 7 Inhibition of JMJD2 induced widespread DNA damage. **a** ACPR cells were treated with CP (10 µM) and/or ML324 (20 µM) or JIB04 (2 µM) for 48 h and then immunostained with anti-γH2AX antibodies (red) and Dapi (blue). The cells were scanned with a confocal microscopy for images. Higher magnification (bottom) and lower magnification (top) were presented for the staining pattern. Percentages of cells with more than three γH2AX foci (**d**) or pan-nuclear staining of γH2AX (**e**) were presented with SD
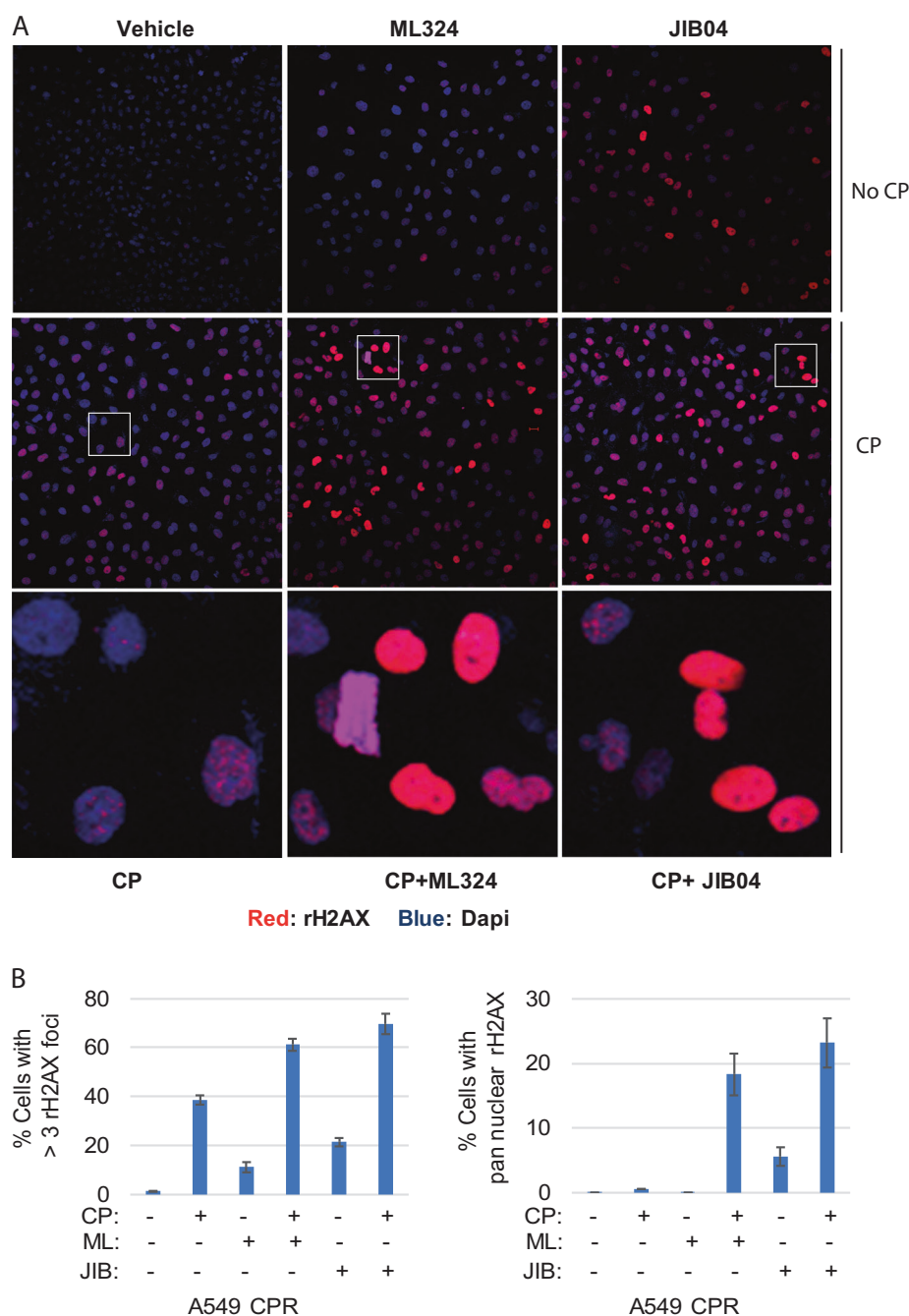
H3K27me3 (a substrate of UTX). Because H3K9me3 and H3K27me3 are markers of compacted heterochromatin [52], CP resistance in cells with increased JMJD2 expression and decreased H3K9me3 and H3K27me3 levels appears to be associated with decreased heterochromatin.

During our studies we have found there is a slight increase in chromatin-association of ATR and Chk1 in response to CP in CP-resistant cells compared to parental controls. JMJD2s appear to be important for ATR and Chk1 association with chromatin since JMJD2 inhibition by ML324 and knockdown of JMJD2B decreased association

of these proteins with chromatin. The association of ATR and Chk1 with chromatin appears important for their activation as inhibition of JMJD2 decreased levels of activated (phosphorylated) ATR and Chk1 and also total Chk1 levels. Dissociation of Chk1 from chromatin leads to its ubiquitination and degradation [41]. JMJD2 inhibition caused a slight increase in the Chk1 ubiquitination and Chk1 association with the ubiquitin ligase Cul4A, suggesting JMJD2 inhibition may reduce Chk1 levels in part via Cul4A-mediated ubiquitination. We speculate JMJD2-mediated demethylation maintains Chk1 stability via chromatin

Fig. 8 Inhibition of cdc7 decreases CP and ML324-induced DNA damage and cell death. **a** A549 and A549CPR (ACPR) cells were treated with CP (10 μM for A549, 20 μM for ACPR) and/or ML324 (20 μM) for 24 h. Lysates were immunoblotted for the indicated proteins. **b** A549 and ACPR cells were treated with CP (10 μM for A549, 20 μM for ACPR) and/or ML324 (20 μM) with or without XL413 (10 μM) for 24 h and then released of CP for 48 h. Cells were analyzed with flow cytometry for cell cycle. Percent sub-G1 cells were presented with SD indicated. There is a significant difference ($p < 0.01$) between CP plus ML324 and CP plus ML324 plus XL413 conditions in both cell lines
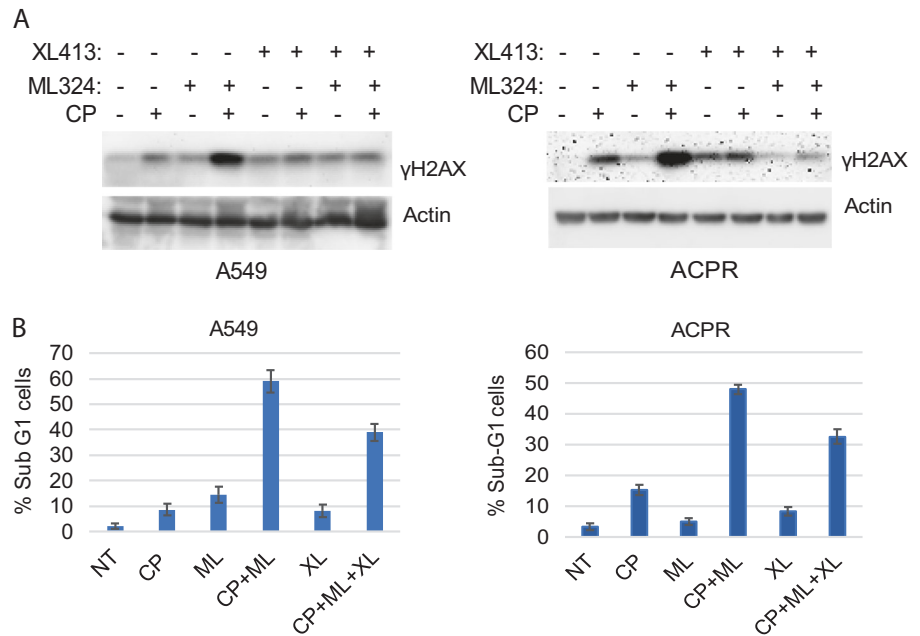
association. Consistent with the effect of JMJD2 inhibition, knockdown of JMJD2A/2B/2D also decreased ATR and Chk1 activation in CP-treated cells. We speculate that JMJD2-regulated decreases in histone methylation may lead to reduced heterochromatin and this, in turn, leads to a more open chromatin structure important for recruitment of ATR, Chk1, and potentially other proteins to DNA damage sites. A previous study showed that JMJD2B plays an important role in repair of heterochromatin in response to DSBs [53]. It will be interesting to know if JMJD2 proteins carry out this function by altering chromatin structure and affecting the recruitment of repair proteins to DSB sites.

In our studies we have noticed that inhibition of JMJD2s or knockdown of JMJD2B only partially sensitized cells to immediate apoptosis by CP. However, long-term survival of CP-treated cells is almost completely suppressed by JMJD2 inhibition or JMJD2B knockdown. In response to replication stress the ATR and Chk1 pathway is important for preventing an accumulation of single-stranded DNA which could deplete RPA and cause irreversible DNA damage [45]. Our results showed that inhibition of JMJD2 led to depletion of RPA2 from cytoplasm and nucleoplasm while increasing chromatin-associated RPA2. Inhibition of JMJD2 increased origin firing and stalled cells in S-phase in CP-treated cells, which may lead to increase in SSDNA and depletion of RPA2. Inhibition of JMJD2 also caused a pronounced increase in γH2AX levels and pan-nuclear immunostained γH2AX. These results are compatible with previous findings that ATR pathway activation prevents depletion of RPA and that inhibition of ATR/Chk1 increases pan-nuclear staining of γH2AX [54–56]. Because CP and ML324 combination induced γH2AX is reversed by

inhibition of cdc7 with XL413 that is shown to suppress origin firing and reverse γH2AX in cells ATR is inhibited [46], and because inhibition of ATR can deplete RPA by increasing origin firing [45], it is likely that inhibition of JMJD2 decreases activation of ATR and Chk1 with a subsequent increase in origin firing, stalled replication, and increased SSDNA and depletion of RPA, leading to widespread DNA DSB in response to CP.

In summary, we identified JMJD2 family demethylases as a novel CP resistance factor in NSCLC cells. We propose JMJD2s decrease H3K9me3 and H3K36me3 levels to promote association of ATR and Chk1 with chromatin important for their activation. Inhibition of JMJD2s may be a strategy to overcome CP resistance in NSCLC cells.

Materials and methods

Cells and reagents

A549, H1703, and H1975 cells were from ATCC. All cell lines were grown in RPMI medium with 10% fetal bovine serum (FBS), penicillin (100 U/mL) and streptomycin (100 μg/mL). Cells were plated 48 h before treatment. Cisplatin was obtained from Sigma-Aldrich (St. Louis, MO, USA). ML324, JIB04, and XL413 were from Selleck Chemicals (Houston, TX, USA).

Immunoblotting

Whole-cell extracts were prepared by scraping cells in RIPA buffer, resolved by sodium dodecyl sulfate

polyacrylamide gel electrophoresis (SDS-PAGE) and transferred to polyvinylidene difluoride membranes (ThermoFisher Scientific, Waltham, MA, USA). Antibodies to H3K4me3 (C42D8), H3K9me2 ((D85B4), H3K9me3 (D4W1U), H3K27me3 (C36B11), H3K36me3 (D5A7), H3 (D1H2), JMJD2A (C70G6), JMJD2B (D7E6), γH2AX (20E3), pATR (T1989) ((58014), pATM (S1981) (D6H9), ATM (D2E2), pChk1 (S345) (133D3), Chk1 (2G1D5), Cul4A (2699) and Rb (4H1) were from Cell Signaling (Boston, MA, USA); β-actin (C4), ATR (N19), and JMJD2C (D4) antibodies were from Santa Cruz (CA, USA). JMJD1A (A301-539A), UTX (A302-374A), and RPA32 (AA300-244A) antibodies were from Bethyl laboratories (Montgomery, TX). JMJD2D antibodies (NBP1-03357APC) are from Novus Biologicals (Centennial CO, USA). Ubiquitin antibodies (13-1600) were from Invitrogen (Carlsbad, CA, USA). Primary antibodies were detected with goat anti-mouse or goat anti-rabbit secondary antibodies conjugated to horseradish peroxidase were from Invitrogen using Immobilon Western HRP Substrate from EMD Millipore (Burlington, MA). Experiments were conducted for three times with one representative presented.

Subcellular protein fractionation

Cells were fractionated for subcellular proteins using Subcellular Protein Fractionation Kit from ThermoFisher Scientific (Waltham, MA). Cytoplasmic and nuclear proteins were isolated following the protocol from the manufacturer. The chromatin fraction was further extracted from nuclear lysates by spinning down with a microcentrifuge at the maximal speed for 5 min. The chromatin was subsequently lysed in RIPA buffer with sonication.

Flow cytometry

For cell cycle analysis, cells were harvested and fixed in 25% ethanol overnight. The cells were then stained with propidium iodide (25 μg/mL, Calbiochem). Flow cytometry analysis was performed on a Gallios™ Flow Cytometer (Beckman Coulter), analyzed with FlowJo 10 (Treestar Inc). For each sample, 10,000 events were collected. Experiments are conducted in triplicate and repeated at least one more time. Average value from one representative experiment is presented with SD indicated as error bars.

Colony formation assay

Cells were plated in six-well plates with 200 cells/well in triplicate for 24 h. Cells were then treated with drugs for 24 h and then released of drugs. Cell were allowed to recover for 3 weeks to form colonies. Colonies were stained with 1% methylene blue (Sigma) in ethanol and number of

positive colonies was counted. Experiments are conducted in triplicate and repeated at least one more time. Average value from one representative experiment is presented with SD indicated as error bars.

siRNA-mediated transient knockdown

JMJD2A/2B/2D siRNA, Chk1 siRNA (On-target plus smart pool), and Control siRNA (On-target plus siControl non-targeting pool) were purchased from GE Dharmacon (Lafayette, CO) and were transfected according to the manufacturer's guidelines using DharmaFECT I reagent.

RNA isolation and real-time quantitative PCR analysis

Total RNA was prepared using Total RNA Mini Kit (IBI Scientific, IA, USA); the first cDNA strand was synthesized using High Capacity cDNA Reverse Transcription Kit (Applied Biosystems, CA, USA). Manufacturers' protocols were followed in each case. PCR primers for histone lysine methyltransferases and demethylases are listed in Tables S1 and S2. PCR primers for Chk1 and β-actin were listed in Table S3. *SYBR* green PCR kit (Midwest Scientific, St. Louis, USA) was used according to the manufacturer's instructions. QuantStudio™ 6 was used as follows: activation at 95 °C; 2 min, 40 cycles of denaturation at 95 °C; 15 s and annealing/extension at 60 °C; 60 s, followed by melt analysis ramping from 60 to 95 °C. Relative gene expression was determined by the $\Delta\Delta C_t$ method using β-Actin to normalize. Experiments are conducted in triplicate and repeated at least one more time. Average value from one representative experiment is presented with SD indicated as error bars.

Confocal immunofluorescence microscopy

For immunofluorescence analysis, cells were cultured on glass coverslips, fixed in 4% formaldehyde/PBS, permeabilized with 0.5% Triton X-100 for 5 min, and stained with anti-γH2AX antibodies followed by Alexa Fluor 564-conjugated secondary Abs. The stained cells were mounted in mounting medium with Dapi (Life Technologies), and images were acquired with a confocal microscope (Zeiss LSM 700) under ×200 or ×400 magnifications.

DNA fiber assays

For determining replication dynamics under nontreated (NT) conditions, cells were incubated with 5-iodo-2′-deoxyuridine (IdU) for 20 min followed by chloro-2′-deoxyuridine (CldU; both from Sigma-Aldrich) for 60 min. To understand the influence of cisplatin (CP), ML324, or

both on the ability of cells to restart replication, cells were incubated with (IdU) for 20 min, treated with cisplatin (CP), ML324, or both for 12 h, followed by CldU for 60 min. DNA fibers were spread on glass slides as described [57]. After methanol/acetic (3:1) fixation for 10 min, cells were washed in distilled H_2O and immersed in 2.5 M HCl for 80 min. After DNA denaturation, slides are washed three times in PBS for 5 min. After DNA denaturation, IdU- and CldU-labeled tracts were detected by 1 h incubation at 37 °C with rat anti-BrdU antibody (dilution 1:500 detects BrdU and CldU; OBT0030, Accurate Chemical Scientific Corporation) and mouse anti-BrdU antibody (1:500, detects BrdU and IdU; BD-347580, Becton Dickinson). Next, slides were incubated for 2 h at 37 °C with Alexa Fluor 594-rabbit anti-mouse (dilution 1:500; A-11062, ThermoFisher Scientific) and Alexa Fluor 488-chicken anti-rat (dilution 1:500; A-21470, ThermoFisher Scientific)). Lastly, slides were incubated for 2 h at 37 °C with Alexa Fluor 594-goat anti-rabbit (dilution 1:1000; A-11037, ThermoFisher Scientific) and Alexa Fluor 488-goat anti-chicken dilution 1:1000; A-11039, ThermoFisher Scientific). Fiber images were acquired by fluorescence microscopy.

At least 1000−2000 fibers and 25 images were scored for each independent experiment. Scoring of fibers was performed using software described previously [58]. The software recognizes the DNA fibers and creates an excel spreadsheet with the raw data. Parameters are then adjusted within the excel file. To set the parameters, an entire independent experiment was scored, and parameters were then set to reflect what was observed. These exact parameters were then applied to each independent experiment. The parameters include a min size of any red or green segment (15 pixels), minimum track length (15 pixels), percent of discontinuity within the track (<30%), number of continuous pixels within a track without a signal (5), a signal to noise ratio threshold (1) and a maximum track thickness (<10 pixels) to avoid scoring bundled DNA fiber. These parameters greatly reduced the number of DNA fiber bundles, background staining and stretched fibers included in the analysis.

Replication restart assay

A549 cells were labeled with 10 µM BrdU for 1 h prior to treatment. Cells were treated with either 10 µM cisplatin or 10 µM cisplatin plus 20 µM ML324 for 6 h. Following treatment, cells were washed three times with PBS and refed with complete media for 6 and 24 h containing 50 µM EdU. Additionally, cells treated with cisplatin plus ML324 were maintained in the presence of 20 µM ML324 for 6 and 24 h. Cells were collected according to the FITC-BrdU Flow Kit (BD Biosciences). Staining for BrdU and EdU were performed according to the FITC-BrdU Flow Kit with the exception that BrdU and EdU were sequentially stained

to maintain proper concentration of antibody needed for adequate staining. Click-iT™ EdU Alexa Fluor™ 647 Flow Cytometry Assay Kit (ThermoFisher Scientific) was used for the staining of EdU according to manufacturer's procEdUre. Detection of BrdU- and EdU-positive cells was performed on a Gallios Flow Cytometer (Beckman Coulter) and analyzed using FlowJo (TreeStar) software. BrdU-positive cells were gated as shown in Fig. S4.

Statistical analysis

One-way analysis of variance (ANOVA) and Student's t test were used to determine the statistical significance of differences among experimental groups. Student's t test was used to determine the statistical significance between the control and experimental groups.

Compliance with ethical standards

References

1. Aggarwal C, Borghaei H. Treatment paradigms for advanced non-small cell lung cancer at academic medical centers: involvement in clinical trial endpoint design. Oncologist. 2017;22:700–8.
2. Johnson DH, Schiller JH, Bunn PA Jr. Recent clinical advances in lung cancer management. J Clin Oncol. 2014;32:973–82.
3. Steuer CE, Behera M, Ernani V, Higgins KA, Saba NF, Shin DM, et al. Comparison of concurrent use of thoracic radiation with either carboplatin-paclitaxel or cisplatin-etoposide for patients with stage III non-small-cell lung cancer: a systematic review. JAMA Oncol. 2016;3:1120–9.
4. Chang A. Chemotherapy, chemoresistance and the changing treatment landscape for NSCLC. Lung Cancer. 2011;71:3–10.
5. Eastman A, Schulte N. Enhanced DNA repair as a mechanism of resistance to cis-diamminedichloroplatinum(II). Biochemistry. 1988;27:4730–4.
6. Kelland LR, Barnard CF, Evans IG, Murrer BA, Theobald BR, Wyer SB, et al. Synthesis and in vitro and in vivo antitumor activity of a series of trans platinum antitumor complexes. J Med Chem. 1995;38:3016–24.
7. Galluzzi L, Senovilla L, Vitale I, Michels J, Martins I, Kepp O, et al. Molecular mechanisms of cisplatin resistance. Oncogene. 2012;31:1869–83.
8. Bhagwat N, Olsen AL, Wang AT, Hanada K, Stuckert P, Kanaar R, et al. XPF-ERCC1 participates in the Fanconi anemia pathway of cross-link repair. Mol Cell Biol. 2009;29:6427–37.
9. Ferry KV, Hamilton TC, Johnson SW. Increased nucleotide excision repair in cisplatin-resistant ovarian cancer cells: role of ERCC1-XPF. Biochem Pharmacol. 2000;60:1305–13.

10. Usanova S, Piee-Staffa A, Sied U, Thomale J, Schneider A, Kaina B, et al. Cisplatin sensitivity of testis tumour cells is due to deficiency in interstrand-crosslink repair and low ERCC1-XPF expression. Mol Cancer. 2010;9:248.

11. Britten RA, Liu D, Tessier A, Hutchison MJ, Murray D. ERCC1 expression as a molecular marker of cisplatin resistance in human cervical tumor cells. Int J Cancer. 2000;89:453–7.

12. Lord RV, Brabender J, Gandara D, Alberola V, Camps C, Domine M, et al. Low ERCC1 expression correlates with prolonged survival after cisplatin plus gemcitabine chemotherapy in non-small cell lung cancer. Clin Cancer Res. 2002;8:2286–91.

13. Mendoza J, Martinez J, Hernandez C, Perez-Montiel D, Castro C, Fabian-Morales E, et al. Association between ERCC1 and XPA expression and polymorphisms and the response to cisplatin in testicular germ cell tumours. Br J Cancer. 2013;109:68–75.

14. Enoiu M, Jiricny J, Scharer OD. Repair of cisplatin-induced DNA interstrand crosslinks by a replication-independent pathway involving transcription-coupled repair and translesion synthesis. Nucleic Acids Res. 2012;40:8953–64.

15. Zhou W, Chen YW, Liu X, Chu P, Loria S, Wang Y, et al. Expression of DNA translesion synthesis polymerase eta in head and neck squamous cell cancer predicts resistance to gemcitabine and cisplatin-based chemotherapy. PLoS ONE. 2013;8:e83978.

16. Cimprich KA, Cortez D. ATR: an essential regulator of genome integrity. Nat Rev Mol Cell Biol. 2008;9:616–27.

17. Kumagai A, Dunphy WG. How cells activate ATR. Cell Cycle. 2006;5:1265–8.

18. Gadhikar MA, Sciuto MR, Alves MV, Pickering CR, Osman AA, Neskey DM, et al. Chk1/2 inhibition overcomes the cisplatin resistance of head and neck cancer cells secondary to the loss of functional p53. Mol Cancer Ther. 2013;12:1860–73.

19. Sangster-Guity N, Conrad BH, Papadopoulos N, Bunz F. ATR mediates cisplatin resistance in a p53 genotype-specific manner. Oncogene. 2011;30:2526–33.

20. Vendetti FP, Lau A, Schamus S, Conrads TP, O'Connor MJ, Bakkenist CJ. The orally active and bioavailable ATR kinase inhibitor AZD6738 potentiates the anti-tumor effects of cisplatin to resolve ATM-deficient non-small cell lung cancer in vivo. Oncotarget. 2015;6:44289–305.

21. Gursoy-Yuzugullu O, House N, Price BD. Patching broken DNA: nucleosome dynamics and the repair of DNA breaks. J Mol Biol. 2016;428:1846–60.

22. Kuo LJ, Yang LX. Gamma-H2AX—a novel biomarker for DNA double-strand breaks. In Vivo. 2008;22:305–9.

23. Turinetto V, Giachino C. Multiple facets of histone variant H2AX: a DNA double-strand-break marker with several biological functions. Nucleic Acids Res. 2015;43:2489–98.

24. Hartlerode AJ, Guan Y, Rajendran A, Ura K, Schotta G, Xie A, et al. Impact of histone H4 lysine 20 methylation on 53BP1 responses to chromosomal double strand breaks. PLoS ONE. 2012;7:e49211.

25. Hsiao KY, Mizzen CA. Histone H4 deacetylation facilitates 53BP1 DNA damage signaling and double-strand break repair. J Mol Cell Biol. 2013;5:157–65.

26. Wakeman TP, Wang Q, Feng J, Wang XF. Bat3 facilitates H3K79 dimethylation by DOT1L and promotes DNA damage-induced 53BP1 foci at G1/G2 cell-cycle phases. EMBO J. 2012;31:2169–81.

27. Sun Y, Jiang X, Xu Y, Ayrapetov MK, Moreau LA, Whetstine JR, et al. Histone H3 methylation links DNA damage detection to activation of the tumour suppressor Tip60. Nat Cell Biol. 2009;11:1376–82.

28. Gong F, Clouaire T, Aguirrebengoa M, Legube G, Miller KM. Histone demethylase KDM5A regulates the ZMYND8-NuRD chromatin remodeler to promote DNA repair. J Cell Biol. 2017;216:1959–74.

29. Hyun K, Jeon J, Park K, Kim J. Writing, erasing and reading histone lysine methylations. Exp Mol Med. 2017;49:e324.

30. Kooistra SM, Helin K. Molecular mechanisms and potential functions of histone demethylases. Nat Rev Mol Cell Biol. 2012;13:297–311.

31. Bannister AJ, Kouzarides T. Regulation of chromatin by histone modifications. Cell Res. 2011;21:381–95.

32. Dinant C, Houtsmuller AB, Vermeulen W. Chromatin structure and DNA damage repair. Epigenetics Chromatin. 2008;1:9.

33. Price BD, D'Andrea AD. Chromatin remodeling at DNA double-strand breaks. Cell. 2013;152:1344–54.

34. Berry WL, Janknecht R. KDM4/JMJD2 histone demethylases: epigenetic regulators in cancer cells. Cancer Res. 2013;73:2936–42.

35. D'Oto A, Tian QW, Davidoff AM, Yang J. Histone demethylases and their roles in cancer epigenetics. J Med Oncol Therapeut. 2016;1:34–40.

36. Agger K, Cloos PA, Christensen J, Pasini D, Rose S, Rappsilber J, et al. UTX and JMJD3 are histone H3K27 demethylases involved in HOX gene regulation and development. Nature. 2007;449:731–4.

37. Ezponda T, Dupere-Richer D, Will CM, Small EC, Varghese N, Patel T, et al. UTX/KDM6A loss enhances the malignant phenotype of multiple myeloma and sensitizes cells to EZH2 inhibition. Cell Rep. 2017;21:628–40.

38. Agger K, Miyagi S, Pedersen MT, Kooistra SM, Johansen JV, Helin K. Jmjd2/Kdm4 demethylases are required for expression of Il3ra and survival of acute myeloid leukemia cells. Genes Dev. 2016;30:1278–88.

39. Northcott PA, Nakahara Y, Wu X, Feuk L, Ellison DW, Croul S, et al. Multiple recurrent genetic events converge on control of histone lysine methylation in medulloblastoma. Nat Genet. 2009;41:465–72.

40. Toyokawa G, Taguchi K, Edagawa M, Shimamatsu S, Toyozawa R, Nosaki K, et al. The prognostic impact of Jumonji domain-containing 2B in patients with resected lung adenocarcinoma. Anticancer Res. 2016;36:4841–6.

41. Zhang YW, Otterness DM, Chiang GG, Xie W, Liu YC, Mercurio F, et al. Genotoxic stress targets human Chk1 for degradation by the ubiquitin-proteasome pathway. Mol Cell. 2005;19:607–18.

42. Hromas R, Williamson EA, Fnu S, Lee YJ, Park SJ, Beck BD, et al. Chk1 phosphorylation of Metnase enhances DNA repair but inhibits replication fork restart. Oncogene. 2012;31:4245–54.

43. Petermann E, Woodcock M, Helleday T. Chk1 promotes replication fork progression by controlling replication initiation. Proc Natl Acad Sci USA. 2010;107:16090–5.

44. Seiler JA, Conti C, Syed A, Aladjem MI, Pommier Y. The intra-S-phase checkpoint affects both DNA replication initiation and elongation: single-cell and -DNA fiber analyses. Mol Cell Biol. 2007;27:5806–18.

45. Toledo LI, Altmeyer M, Rask MB, Lukas C, Larsen DH, Povlsen LK, et al. ATR prohibits replication catastrophe by preventing global exhaustion of RPA. Cell. 2013;155:1088–103.

46. Mutreja K, Krietsch J, Hess J, Ursich S, Berti M, Roessler FK, et al. ATR-Mediated global fork slowing and reversal assist fork traverse and prevent chromosomal breakage at DNA interstrand cross-links. Cell Rep. 2018;24:2629–42 e2625.

47. Dasari S, Tchounwou PB. Cisplatin in cancer therapy: molecular mechanisms of action. Eur J Pharmacol. 2014;740:364–78.

48. Basu A, Krishnamurthy S. Cellular responses to Cisplatin-induced DNA damage. J Nucleic Acids. 2010;2010:201367.

49. Nam EA, Cortez D. ATR signalling: more than meeting at the fork. Biochem J. 2011;436:527–36.

50. Li CC, Yang JC, Lu MC, Lee CL, Peng CY, Hsu WY, et al. ATR-Chk1 signaling inhibition as a therapeutic strategy to enhance cisplatin chemosensitivity in urothelial bladder cancer. Oncotarget. 2016;7:1947–59.

51. Mallette FA, Mattiroli F, Cui G, Young LC, Hendzel MJ, Mer G, et al. RNF8- and RNF168-dependent degradation of KDM4A/JMJD2A triggers 53BP1 recruitment to DNA damage sites. EMBO J. 2012;31:1865–78.

52. Saksouk N, Simboeck E, Dejardin J. Constitutive heterochromatin formation and transcription in mammals. Epigenetics Chromatin. 2015;8:3.

53. Zheng H, Chen L, Pledger WJ, Fang J, Chen J. p53 promotes repair of heterochromatin DNA by regulating JMJD2b and SUV39H1 expression. Oncogene. 2014;33:734–44.

54. Andrade-Lima LC, Andrade LN, Menck CF. ATR suppresses apoptosis after UVB irradiation by controlling both translesion synthesis and alternative tolerance pathways. J Cell Sci. 2015;128:150–9.

55. Gagou ME, Zuazua-Villar P, Meuth M. Enhanced H2AX phosphorylation, DNA replication fork arrest, and cell death in the absence of Chk1. Mol Biol Cell. 2010;21:739–52.

56. Sanjiv K, Hagenkort A, Calderon-Montano JM, Koolmeister T, Reaper PM, Mortusewicz O, et al. Cancer-specific synthetic lethality between ATR and CHK1 kinase activities. Cell Rep. 2016;14:298–309.

57. Chastain PD 2nd, Brylawski BP, Zhou YC, Rao S, Chu H, Ibrahim JG, et al. DNA damage checkpoint responses in the S phase of synchronized diploid human fibroblasts. Photochem Photobiol. 2015;91:109–16.

58. Steward O, Popovich PG, Dietrich WD, Kleitman N. Replication and reproducibility in spinal cord injury research. Exp Neurol. 2012;233:597–605.